ScienceDirect

Science of The Total Environment
Volume 825, 15 June 2022, 154087

Vulnerability and driving factors of soil inorganic carbon stocks in Chinese croplands

Jingjing Tao [a 1], Sajjad Raza [a 1], Mengzhen Zhao [a], Jiaojiao Cui [a], Peizhou Wang [a], Yueyu Sui [b], Kazem Zamanian [c], Yakov Kuzyakov [c d], Minggang Xu [e], Zhujun Chen [a] ✉, Jianbin Zhou [a] ✉

Show more

Outline | Share | Cite

https://doi.org/10.1016/j.scitotenv.2022.154087
Get rights and content

Highlights

- Chinese croplands have lost SIC stocks by 27–38% during the past 30 years.
- Soil pH has decreased by 0.53 units over the past 30 years.
- Nitrogen fertilization and water balance are the main drivers of SIC losses.
- Balanced N fertilization and irrigation are recommended to avoid soil degradation.

Abstract

The long-term stability of soil inorganic carbon (SIC) and its minimum contribution towards global C cycle has been challenged, as recent studies have showed rapid decreases in SIC stocks in intensive agricultural systems. However, the extent of SIC losses and its driving factors remains unclear. Here, we compared changes in SIC density (SICD) in Chinese croplands between the 1980s and 2010s. The SIC contents in 1980s were obtained from second national soil survey (n = 949) and published studies (n = 47). The SIC contents in 2010s were based on resampling of soil profiles from the same locations during 2019 and 2020 (n = 30), as well as data from published studies and national soil survey (n = 903). We found that Chinese croplands have lost 27–38% of SICD from the 0–40 cm soil layer and that the soil pH has decreased by 0.53 units over the past 30 years. These SIC losses increased with the ratio of precipitation (P) to potential evapotranspiration (PET) and most notably with nitrogen (N) fertilization. The SICD decreased greatly in humid and semiarid regions, and these losses were enhanced by high N fertilization rates; however, the SICD increased in very arid regions. This analysis demonstrates that the water balance and N fertilization are major drivers leading to dramatic losses of SICD in croplands and, consequently, to decreases in soil fertility and functions.

Graphical abstract

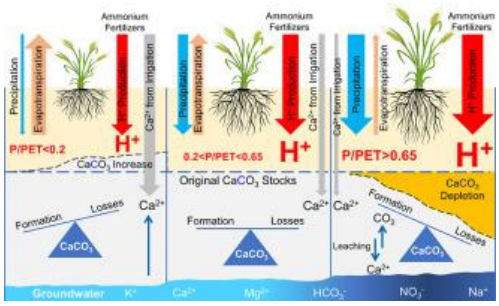

Download : Download high-res image (190KB)

Download : Download full-size image

Previous Next

Keywords

Soil inorganic carbon density; Soil acidification; Greenhouse gases; Water balance; Nitrogen fertilization; Carbon cycle

1. Introduction

Soil carbon (C) comprises organic carbon (SOC) and inorganic carbon (SIC). The role of SOC in C sequestration is well known and has received widespread attention (Loisel et al., 2019; Hein et al., 2020; Post and Kwon, 2000), but our understanding of SIC dynamics and its contribution towards climate change is still rudimentary. Globally, SIC stocks in the upper 1 m soil profile are 695–800 Pg (Schlesinger, 1982; Batjes, 1996); those in the upper 2 m reach 2250 Pg. SIC exists mainly in the form of $CaCO_3$ and is the main C pool in arid and semiarid regions, where it accounts for 90% of the total soil C stocks (Filippi et al., 2020). Historically, it has been accepted that SIC is very stable, for periods of over 85,000 years, and that it therefore has a limited role in the global C cycle (Schlesinger, 1985). Consequently, the contributions of SIC to climate change and C sequestration have been disregarded. This stability and the very slow contribution of SIC to the global C cycle is common only in natural ecosystems in semiarid and arid areas, and the situation changes completely under intensive crop production.

SIC is important for the physical, chemical and (micro)biological properties of soil, its accelerated losses threaten long-term soil health, crops productivity, and ecological services (Raza et al., 2020). SIC accumulation and distribution with depth depend initially on soil parent material and are affected during pedogenesis by (i) climatic conditions, such as precipitation and temperature, which affect evapotranspiration (Yang et al., 2010; Raheb et al., 2017); (ii) soil properties, such as CO_2 partial pressure, pH, texture, and cation exchange capacity (Zamanian et al., 2016a, Zamanian et al., 2016b; An et al., 2019); (iii) source of Ca^{2+} and Mg^{2+} (Monger et al., 2015), and (iv) vegetation or crops. Water balance defined as the ratio of water input (precipitation + irrigation in croplands) and output (evapotranspiration + runoff) is the main driver of (re)distribution of the pedogenic carbonate content in soil (Quade and Cerling, 1990; Gocke and Kuzyakov, 2011). A positive water balance (surplus of water) results in the drainage of water that leaches cations and anions. Carbonate dissolution in water, especially when it is enriched with CO_2, results in the release of HCO_3^-, Ca^{2+} and Mg^{2+}. The dissolved ions may move downward and reprecipitate as carbonate when a calcite solubility constant is achieved or may be leached out of the soil to groundwater (Gile et al., 1966; Li et al., 2017). SIC stocks in rain-fed and irrigated croplands decreased within 30–100 years after land-use change from natural vegetation; the ^{13}C tracing approach further showed that the SIC turnover rate was faster (30–100 years after land use change) in croplands and that even deeper than 4.9 m SIC stocks were affected (Kim et al., 2020). The total precipitation and the frequency of extreme precipitation events are projected to increase in the 21st century due to climate change (Sinha et al., 2017); this could potentially accelerate alteration of SIC stocks regionally and globally. Hence, the impact of water-change patterns as a potential driver of SIC stocks deserves attention.

Soil acidification is another major factor influencing SIC stocks (Shi et al., 2012; Raza et al., 2020; Zamanian et al.,

2018). Natural soil acidification occurs over centuries and millennia; therefore, the corresponding carbonate dissolution and losses are very slow (Raza et al., 2021a). Global nitrogen (N) flows have currently exceeded the planetary threshold, primarily as the result of industrial NH_3 production and use for fertilization, cultivation of N-fixing crops (legumes), and the combustion of fossil fuels (Fowler et al., 2013; Steffen et al., 2015). China consumes approximately 30% of global N fertilizers, mainly as ammonium (NH_4^+)-based fertilizers. The soil acidification caused by nitrification is much stronger than the acidity induced by N deposition, root exudation and other factors (Guo et al., 2010). The loss of carbonates from surface soil is one of the serious consequences of acidification (Kuzyakov et al., 2021; C. Wang et al., 2015; Zamanian et al., 2018; Zamanian and Kuzyakov, 2019). The labeling of $CaCO_3$ with ^{13}C showed that NH_4^+ fertilization increased SIC-derived CO_2 emissions (Bramble et al., 2020). The grasslands in China lost 0.027 kg C m^{-2} yr^{-1} of SICD (SIC density) from the 0–10 cm soil layer due to atmospheric N deposition and acid deposition (Yang et al., 2012). Similarly, acidification induced by shrub encroachment in the grasslands of Inner Mongolia caused a loss of 19% of SIC stocks in the upper 1 m soil profile; and SIC was mainly dissolved and lost as CO_2 to the atmosphere (Liu et al., 2020). The rate of $CaCO_3$ loss from cultivated soil is faster than that in natural soil (Kim et al., 2020). Field-scale (Poulton, 1996), regional (Raza et al., 2020) and global (Zamanian et al., 2018) studies clearly showed that anthropogenic activities involving excessive N fertilization, irrigation, and acid deposition in intensive agricultural systems have rapidly changed SIC stocks, especially those in the topsoil.

The SIC stocks in the upper 1 m profile in China have been estimated to be 78 Pg C (Li et al., 2007), and are vulnerable to losses by intensive agricultural practices. Based on theoretical calculations of acidification induced by N fertilization, previous studies have found that SIC losses are taking place rapidly worldwide and in China (Zamanian et al., 2018; Raza et al., 2020). Chinese croplands have lost 7% of SIC stocks (0.15 Pg C, 1.1 Mg C ha^{-1}) in the past 40 years (1980–2020), and this percentage may increase to 37% by 2100 (Raza et al., 2020). However, these estimations ignored the following processes: (1) the formation of carbonates from dissolved Ca^{2+} and/or Mg^{2+} (Zamanian et al., 2016a; Lu et al., 2020; Wang et al., 2014); (2) the influence of precipitation/irrigation (i.e., water balance) on $CaCO_3$ dissolution, base cations leaching, and soil acidification (Slessarev et al., 2016; Rowley et al., 2020). Therefore, the estimated SIC losses throughout China may not represent the actual field conditions. Therefore, knowing the extent of SIC losses and its driving factors are important topics to be addressed.

This paper hypothesizes that SIC stocks are vulnerable and that losses are accelerated by anthropogenic factors such as acidification induced by spatial water balance (P/PET) and N fertilization (especially ammonium fertilizers). The changes in SICD (SIC density) over the past 30 years were estimated based on measurements of SIC stocks taken during large-scale field campaigns and published literature from the 1980s and 2010s and correlated with concurrent changes in P (precipitation), PET (potential evapotranspiration) and N fertilization.

2. Materials and methods

2.1. Research methodology

This study considered changes in SICD at 0–20 cm and 20–40 cm soil depths because: 1) N fertilization is usually distributed by tillage up to 0–40 cm depth, 2) N is mobile, its transformations and resulting H^+ release can easily reach up to 40 cm depth, 3) root growth and nutrient absorption mostly take place within these layers, 4) climatic conditions such as temperature and rainfall mainly affect the upper soil layers, and 5) most of the available data reported changes in SIC in these layers (Zhao et al., 2020; Gai et al., 2018; Han et al., 2018; Hao et al., 2019). During the 1980s (1980–1990), data on the SIC ($CaCO_3$) contents and other relevant factors from the 0–20 cm and 20–40 cm layers of 949 soil profiles were collected from the Second National Soil Survey of China (NSSO, 1994). Detailed SIC data from another 47 soil profiles were extracted from published studies (Supplementary Information). This brought the total number of data points to 996, covering 22 provinces and autonomous regions, 10 soil classes and 31 soil types. The collected data included information about location, latitude and longitude, soil type, soil depth (cm), $CaCO_3$ (g kg^{-1}), pH, bulk density (g cm^{-3}), organic matter (g kg^{-1}), and soil texture (gravel >2 mm, sand 0.02–2 mm, silt 0.002–0.02 mm, and clay <0.002 mm). The missing bulk density data were calculated according to the following equation (Eq. (1)).

$$BD = -0.123 \times \ln(SOC) + 1.29 \quad (1)$$

where BD is the soil bulk density (g cm^{-3}) and SOC is the soil organic carbon (g kg^{-1}) (Wu et al., 2009).

The data on $CaCO_3$ contents in soils and other properties in the 2010s (2010–2020) included the following: (1) data from the resampling of soil profiles in 2019–2020 at the same locations sampled in the 1980s. The resampling of soil profiles was performed in a north-south transition area in China (Henan and Anhui provinces) and on the Shandong Peninsula. We expected that this area would be a hotspot for SIC losses, as it originally had low SIC stocks (NSSO, 1994) and high rainfall. The latter could further accelerate SIC losses through leaching. Some of the 1980s sampling points just have the information of administrative geographic locations and did not have the actual longitude and latitude information. Therefore, to ensure that the resampling points accurately represented the original locations, four samples were taken around a 2 km radius from where the original samples were taken in the 1980s, and the average value of the four samples was used to correspond to one sampling point in the 1980s. This brought the number of resampled data points to 30 (14 in Henan Province, 5 in Shandong Province, and 11 in Anhui Province).

The method of $CaCO_3$ determination was kept consistent with the method used in the Second National Soil Survey in 1980s (NSSO, 1994). $CaCO_3$ was measured by the manometric collection of CO_2 evolved after HCl (4 mol L^{-1}) addition (Wu et al., 2009).

(2) In addition to the soil resampling, the 2010s data also included 475 soil profiles obtained from the Chinese Soil Series Survey (Chinese Soil Series) and 428 soil profiles obtained from the published literature (Supplementary Information Table S1), bringing the total number of data points in 2010s to 933.

Since the SIC density (SICD) is a unified benchmark for calculating SIC content, and to allow comparisons with other studies, all SIC data were expressed as the SICD. The SICD content was calculated using the following formula (Eq. (2)):

$$\mathbf{SICD} = \Sigma[\mathbf{d} \times \mathbf{BD} \times \mathbf{SIC} \times (\mathbf{1} - \mathbf{R})/\mathbf{100}] \quad (2)$$

where SICD is the soil inorganic carbon density (kg C m^{-2}) at 0–40 cm depth; d is the soil depth (cm); BD represents the soil bulk density (g cm^{-3}); SIC is the soil inorganic carbon content (g C kg^{-1}); and R is the corresponding gravel content of each soil layer (>2 mm; %). SIC is composed mainly of $CaCO_3$, and other types of carbonates account for a very small proportion, so the constant 0.12 was used to convert $CaCO_3$ values to SIC (Yang et al., 2012; Wang et al., 2013; Tan et al., 2014).

The changes in SICD (ΔSICD) and pH (ΔpH) in the 1980s and 2010s were calculated using Eqs. (3), (4), respectively:

$$\Delta\mathbf{SICD} = \mathbf{SICD_{2010s}} - \mathbf{SICD_{1980s}} \quad (3)$$

where ΔSICD is the SICD change between the 1980s and 2010s (kg C m^{-2}), and $SICD_{2010s}$ and $SICD_{1980s}$ are the SICD contents (kg C m^{-2}) in the 2010s and 1980s, respectively.

$$\Delta\mathbf{pH} = \mathbf{pH_{2010s}} - \mathbf{pH_{1980s}} \quad (4)$$

where ΔpH is the pH change between the 1980s and 2010s, and pH_{2010s} and pH_{1980s} are the pH values in the 2010s and 1980s, respectively.

This study used two methods to compare the changes in SICD and pH in different years. The first was the comparison of all measured and collected data points from both time periods (1980s and 2010s). Second, differences in the distribution of data points, climatic conditions, soil types and parent materials that may have affected the results of SICD change were considered. Therefore, 236 paired data points from the same locations with one-to-one correspondence were established to provide better analyses and comparisons (Fig. S1).

2.2. Rainfall, potential evapotranspiration and N fertilization

SIC is affected mainly by water balance and N-induced acidification. The water balance is driven by precipitation (P) and potential evapotranspiration (PET). Therefore, the P/PET ratio was used to reflect the soil water balance. Climate zones are commonly separated into four regions based on their P/PET value: arid (0–0.2), semiarid (0.2–0.5), subhumid (0.5–0.65), and humid (>0.65) (UNESCO, 1979; Yang et al., 2005; Jones and Reid, 2001). The humid region was further subdivided into humid (0.65–1.1) and very humid regions (1.1–2). Data on precipitation were collected from the National Meteorological Data Center (NMDC, 2019), from 839 meteorological monitoring stations distributed nationwide from 1980 to 2015. Precipitation data for the sampling points were obtained from 839 stations using mask

extraction following the ordinary kriging interpolation method in ArcMap. The PET of each site was calculated using ET_0 Calculator Version 3.2 (FAO) software according to the Penman-Monteith formula. Then, ordinary kriging interpolation and mask extraction were performed in ArcMap to obtain the PET data for each sample.

The cumulative N fertilizer input to croplands for each province from 1980 to 2015 was obtained from the National Bureau of Statistics of China (NBSC, 2016).

2.3. Data processing and analysis

Two-sample Kolmogorov-Smirnov (K-S) statistics were calculated to test whether two samples were from the same population when the sample size was more than 30, and the Mann-Whitney *U* test was used when the sample size was below 30. The significance of the changes in SICD and pH was calculated using a paired *t*-test. All statistical analyses were performed using SPSS 21 software. Figures were drawn using OriginPro 2018, and maps were drawn in ArcMap 10.3. The relationships between P/PET, N input, pH and SICD were evaluated through regression.

3. Results

3.1. Changes in soil inorganic carbon density (SICD) and soil pH over 30 years

The spatial and temporal analysis of large number of data points (~2000) showed that SICD in the Chinese croplands have strongly decreased within the past 30 years (Fig. 1). The average SICD of Chinese croplands (0–20 cm and 20–40 cm depth) were 1.90 kg C m^{-2} and 2.13 kg C m^{-2} in the 1980s, decreased by 38% (1.18 kg C m^{-2}) and 27% (1.56 kg C m^{-2}) in the 2010s, respectively (Fig. 2). The SICD of 60% of the sampled soils (top 20 cm) was on average 1.08 kg C m^{-2} in the 1980s and decreased to 0.52 kg C m^{-2} in the 2010s (Fig. 2a). The SICD content at 20–40 cm at 60% of the data points also decreased from 1.23 kg C m^{-2} (1980s) to 0.82 kg C m^{-2} (2010s) (Fig. 2b). The strongest SICD decreases were mainly in Northeast China, the Shandong Peninsula, central and southern Henan, southern Shaanxi, Anhui, Jiangsu, Zhejiang and Sichuan. The decrease was more prominent in the top 20 cm of soils (Fig. 1).

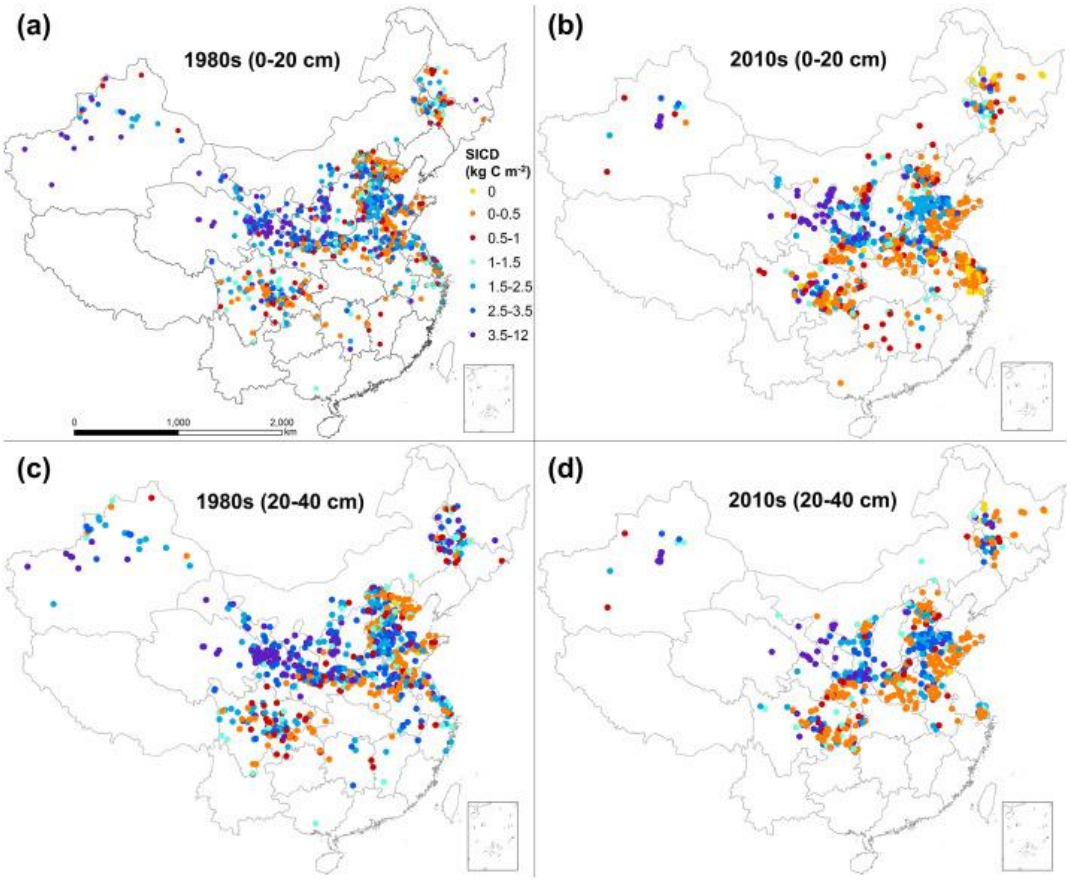

Download : Download high-res image (1MB)

Download : Download full-size image

Fig. 1. Soil inorganic carbon density (SICD, kg C m^{-2}) in Chinese croplands in the 1980s (n = 996) and 2010s (n = 933). Subfigures a and b show SICD at 0–20 cm, and c and d show SICD at 20–40 cm depth.

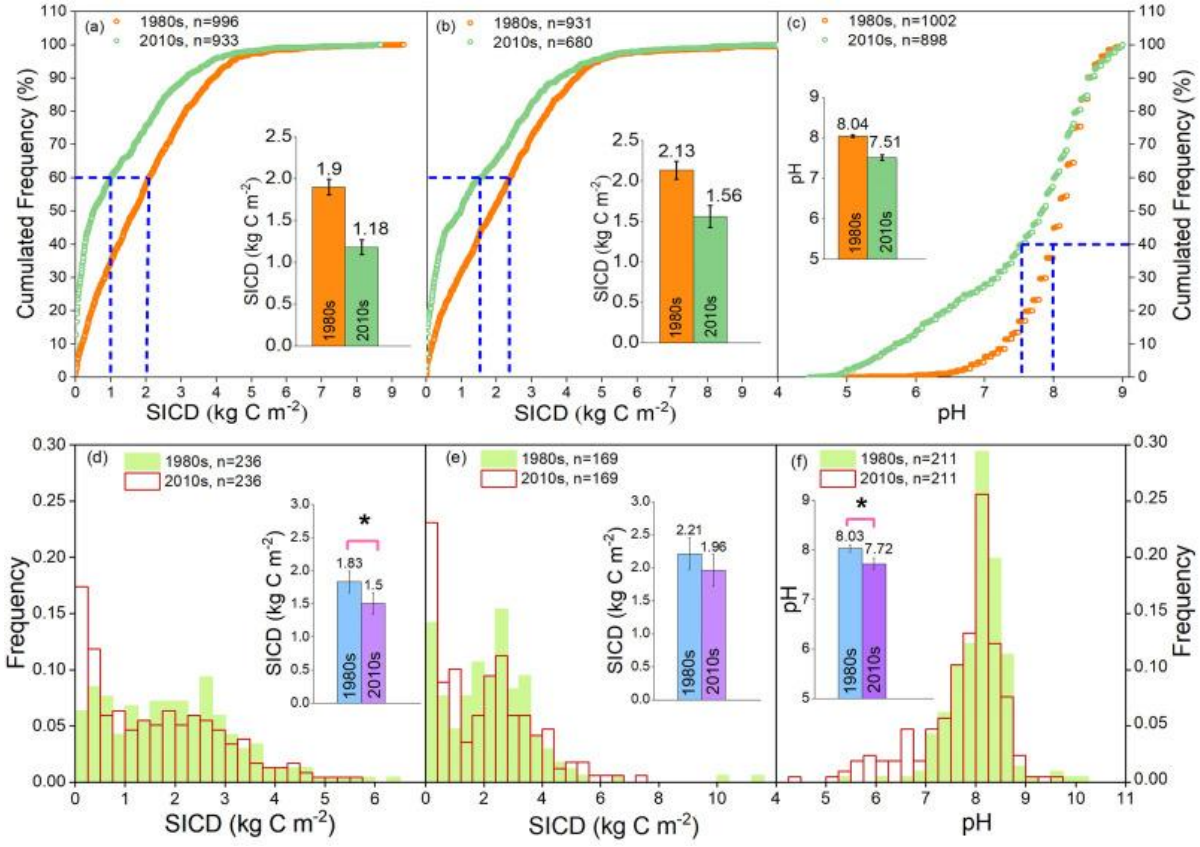

Download : Download high-res image (1MB)

Download : Download full-size image

Fig. 2. Cumulated frequency (%) of soil inorganic carbon density (SICD, kg C m^{-2}) and soil pH in the 1980s (orange dots) and 2010s (green dots) (subfigures a–c). The interior bar graphs show the cumulative SICD. Subfigures a and b show the relationship between the cumulative probability and SICD in the 0–20 cm and 20–40 cm soil layers, respectively. Subfigure c shows the changes in the cumulative probability of soil pH values at 0–20 cm depth. Significant differences in SICD and pH were calculated using a two-sample K-S test at $\alpha = 0.001$. The blue dashed lines show the SICD at 60% of data points in subfigures a and b. The area between the two curves shows the losses of SIC or the pH decrease (acidification) from the 1980s to 2010s. The blue dashed lines in subfigure c show the pH of 40% of the data points. The subfigures d-f show frequency distribution of SICD, kg C m^{-2} among paired data points in the 1980s (green filled) and 2010s (bars with red outline). The interior bar graphs show SICD (kg C m^{-2}) in the 1980s and 2010s. The * shows a significant difference between the two time periods at $\alpha = 0.05$. Subfigure f shows the pH frequency distribution in the 0–20 cm layer in both time periods.

The distribution frequency of high SICD levels at the 236 paired data points decreased from the 1980s to 2010s, while the frequency of low SICD content increased (Fig. 2d). The frequencies of SICD in the 0–20 cm and 20–40 cm soil layers decreased by 18% and 11.3%, respectively (Fig. 2d, e).

The average soil pH of Chinese croplands (0–20 cm) was 8.04 in the 1980s but decreased by 0.53 units to 7.51 in the 2010s. The soil pH of 40% of the sampled soils was below 8.0 in the 1980s and decreased to 7.53 in the 2010s (Fig. 2c). Out of 211 paired data points, a pH decrease of more than 1.0 units was observed at 33 data points (Fig. 2f).

3.2. Relationship between soil inorganic carbon density and pH changes

After 30 years, the changes in pH and SICD in the top 20 cm at the paired data points were directly proportional ($p < 0.01$; Fig. S2a). There was a positive exponential relationship between the pH changes over 30 years and the initial SICD

content in the 1980s (Fig. S2b). The pH decreased sharply in the soils with low SICD (<1.0 kg C m^{-2}), but the pH remained stable when the SICD contents were higher than 3.5 kg C m^{-2} (Fig. S2b).

3.3. Relationship between pH, soil inorganic carbon density and water balance

Soil pH decreased significantly at 0–20 cm depth with the P/PET increase throughout China and in various soil types from the 1980s to the 2010s (Figs. 3, S3). The highest pH decrease (0.72–0.91) was observed in semiarid and humid regions (P/PET: 0.65–2.0), and pH remained generally stable (difference of 0.05 units) under arid conditions (P/PET <0.2) (Fig. 4a). The ΔpH decreased with increase in P/PET (Fig. 4b).

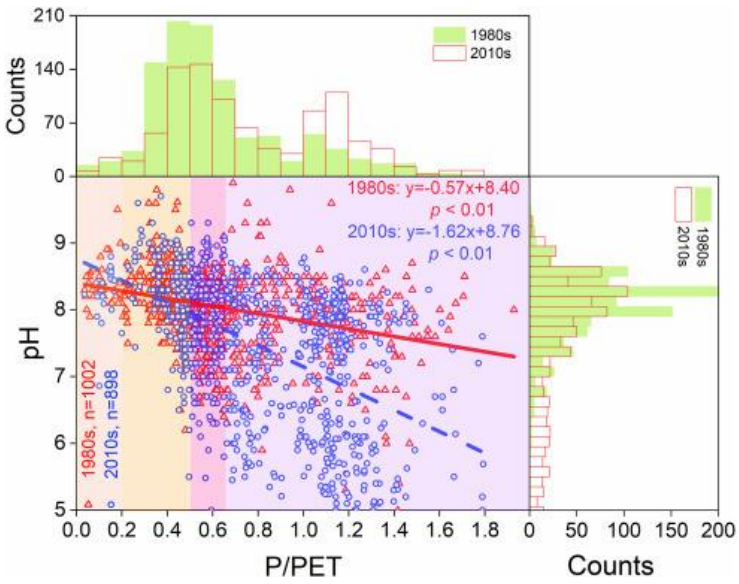

Download : Download high-res image (892KB)

Download : Download full-size image

Fig. 3. Relationship between soil pH and water balance (P/PET) at 0–20 cm soil depth in the 1980s and 2010s. The red and blue colored bullets and lines represent data points and linear regression lines, respectively. The background colors show the gradient of climate types from arid to humid. The yellow background represents an arid climate, the dark yellow background represents a semiarid climate, and the pink and purple background colors represent semihumid and humid climates, respectively. The bar graph above shows the probability distribution of the water balance in 1980 and 2010. The bar graph on the right shows the probability distribution of pH levels.

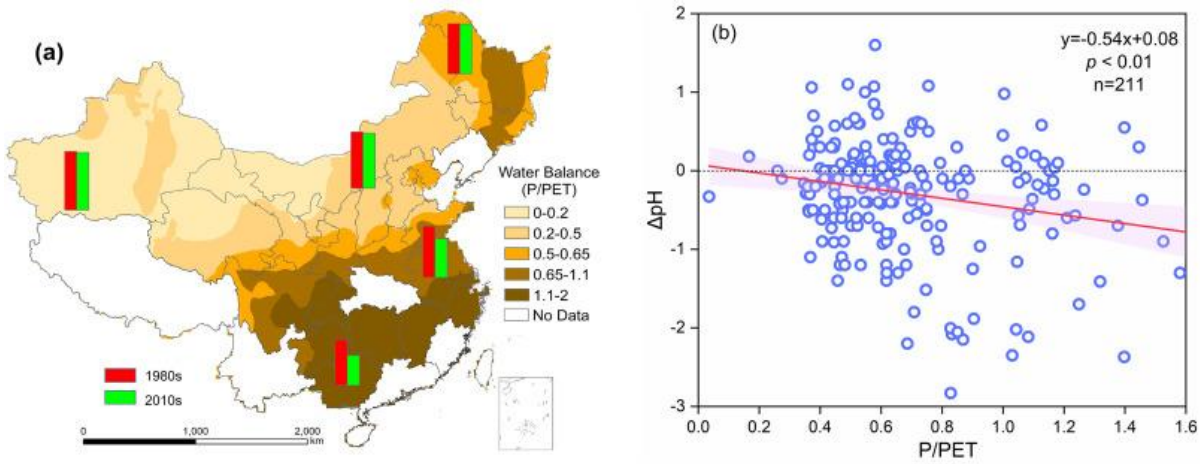

Download : Download high-res image (635KB)

Download : Download full-size image

Fig. 4. Relationship between soil pH at 0–20 cm and water balance (precipitation/potential evapotranspiration, P/PET) in the 1980s and 2010s. The subfigure a shows map of the water balance (P/PET) in the regions. The upper bar graphs

show the pH values in the 1980s (red) and 2010s (green). The scale of pH in each bar is from 5 to 8.4. Subfigure b shows the relationship between pH changes and water balance (P/PET) among paired data points from croplands in China at the 0–20 cm soil layer. The red line is the linear regression line.

SICD strongly decreased with the increase in P/PET from the northwest to the southeast (Fig. 4, Fig. 5). The magnitude of the SICD decrease increased 1) with the water balance (P/PET) value, which was highest in the southeast, and 2) at locations with low carbonate stocks (Fig. 5). The SICD decreased in all regions except in arid climate regions (P/PET <0.2). The maximum SICD decrease was observed in humid regions (P/PET >0.65) at both soil depths, while SICD increased in areas with the lowest P/PET (0–0.2) (Fig. 6a). The ΔSICD values in all soil types significantly decreased with an increase in P/PET (Fig. S4a, b).

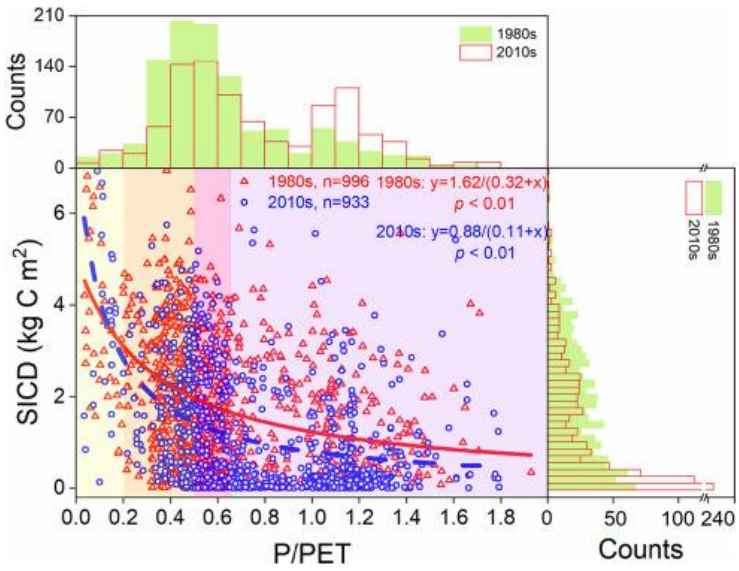

Download : Download high-res image (451KB)

Download : Download full-size image

Fig. 5. Relationship between soil inorganic carbon density (SICD, kg C m^{-2}) and water balance (precipitation/potential evapotranspiration, P/PET) in the 1980s and 2010s. The red and blue colored bullets and lines represent data points and regression lines, respectively. The background colors show the gradient of climate types from arid to humid. The yellow background represents an arid climate, the dark yellow background represents a semiarid climate, and the pink and purple background colors represent semihumid and humid climates, respectively. The bar graph above shows the number of samples depending on the water balance levels. The bar graph on the right shows the number of samples depending on the SICD level. Note the scale break for the counts of the frequency distributions of SICD.

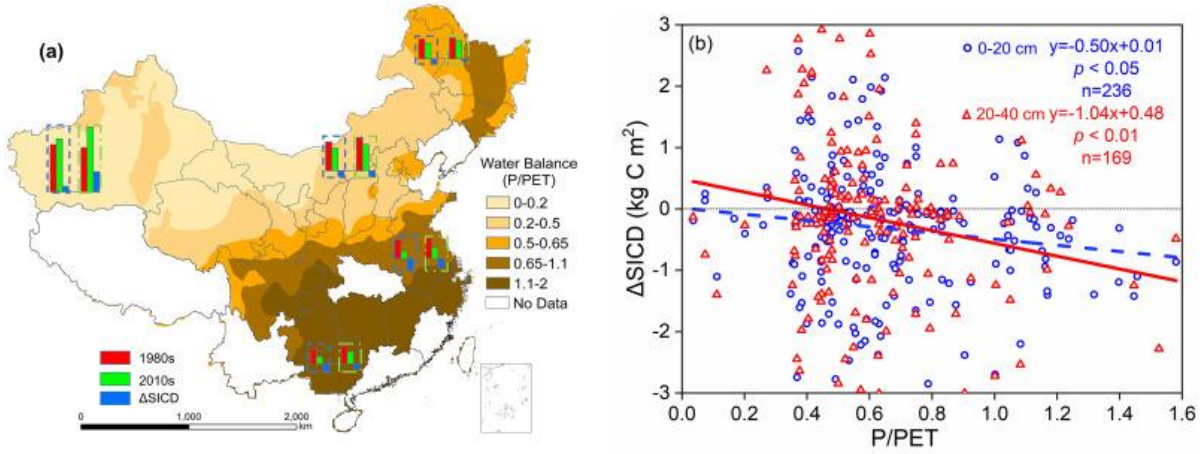

Download : Download high-res image (781KB)

Download : Download full-size image

Fig. 6. Relationship between soil inorganic carbon density (SICD, kg C m^{-2}) and water balance (precipitation/potential evapotranspiration, P/PET) in the 1980s and 2010s. Figure a shows a water balance (P/PET) map of China. The upper bar graphs show the SICDs in the 1980s (red) and 2010s (green) and their difference (2010s–1980s; blue). Figure b shows the relationship between SICD changes (ΔSICD, kg C m^{-2}) and water balance (P/PET) among paired data points from croplands in the 0–20 cm (blue) and 20–40 cm (red) soil layers. The blue and red lines are linear regression lines.

3.4. Relationship between soil pH, inorganic carbon density and nitrogen fertilization

The cumulative N input acidified soils in all provinces except Heilongjiang, Jilin and Sichuan provinces (25 out of 34 provinces) ($p < 0.05$; Fig. 7e). The ΔpH values decreased in all soil classes (Gleysols and Cambisols, Leptosols, Kastanozems, Luvisols, Calcisols, and Anthrosols) except Solonchaks and Lixisols ($p < 0.05$, Fig. S5). The pH changes were unaffected by the N input in arid and semiarid climates, but in the humid and semihumid climate areas, acidification strongly increased with N input ($p < 0.05$; Fig. S6).

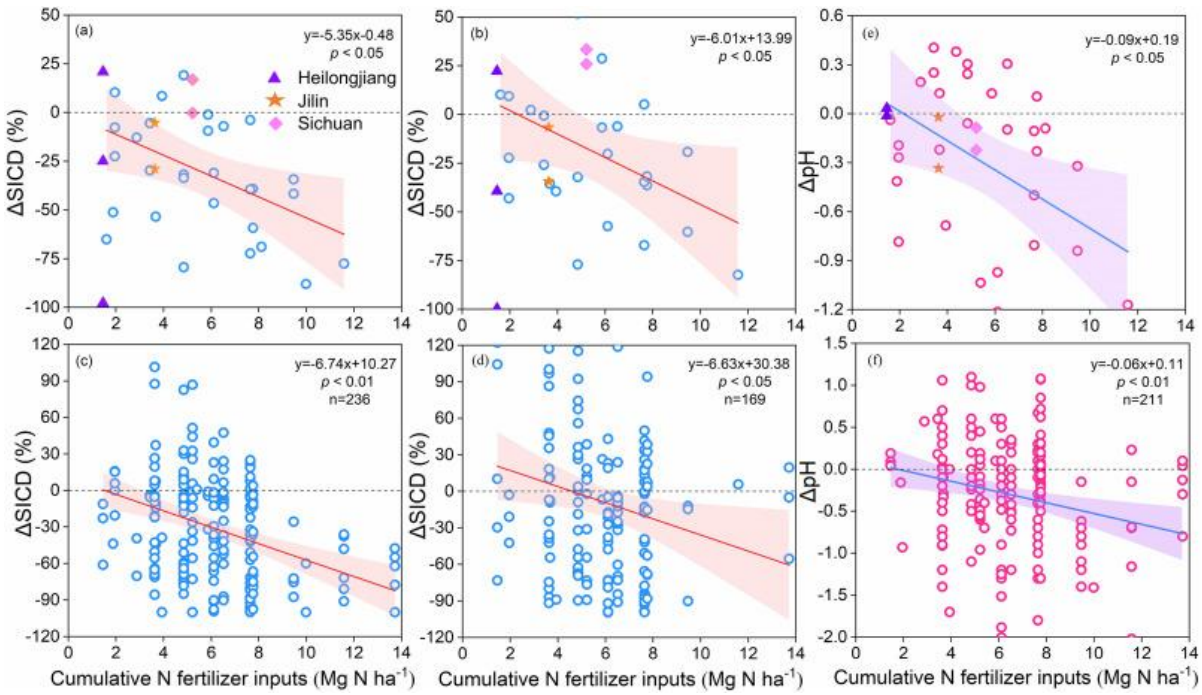

Download : Download high-res image (1MB)

Download : Download full-size image

Fig. 7. Relationship between cumulative N fertilizer input (Mg N ha^{-1}) and SICD changes (ΔSICD, %) (subfigures a, b, c, and d) and soil pH (subfigures e and f) in the 1980s and 2010s. Subfigures a and b show the relationship between cumulative N inputs and ΔSICD among unpaired data points in the 0–20 cm and 20–40 cm soil layers, respectively, and subfigures c and d show the relationship between cumulative N input and SICD among paired data points. Figures e and f show the relationship between cumulative N input and pH in the 0–20 cm soil layer among unpaired and paired data points, respectively. The bullets in Figures a, b and e represent the SICD in regions with variable water balance (P/PET). Triangles represent Heilongjiang Province, stars represent Jilin Province, and squares represent Sichuan Province. The continuous lines among data points in each figure are linear regression lines. The shaded area is the 95% confidence interval.

An increase in the cumulative N input decreased SICD in all provinces except Heilongjiang, Jilin and Sichuan ($p < 0.05$, Fig. 7a, b), and this decrease was more evident in the paired data points (Fig. 7c, d). Excluding those for Solonchaks (electrical conductivity >4 dS m^{-1}), Gleysols, and Cambisols, the ΔSICD values for most soil types (Cambisols, Leptosols, Kastanozems, Luvisols, Calcisols, Anthrosols, and Ferralsols) decreased with increasing N input ($p < 0.05$; Fig. S7).

4. Discussion

4.1. Changes in the soil pH and inorganic carbon density of Chinese croplands

The average soil pH of Chinese croplands has decreased by 0.53 units in the past 30 years ($p < 0.05$; Fig. 2c). Accelerated soil acidification driven by N input decreased pH by 0.26 units globally in the past 30 years (Tian and Niu, 2015) and by 0.13–0.80 units in major Chinese croplands (more prominently in the southwest, south and northeast regions of China and less prominently in the northwest) (J.H. Guo et al., 2010). The decreases in pH were dramatic in intensive agricultural systems, by 1.0–2.0 units within 20–25 years, mainly due to the low soil buffering capacity and high N fertilizer inputs (Zeng et al., 2017; Xie et al., 2019). Compared to cereals, pH decrease has been especially rapid in cash crops (fruits and vegetables) because N fertilization rate is quite high in such crops (Guo et al., 2010). Traditional flooding irrigation and excessive fertilization for 5 years decreased pH by 0.06–0.73 units in intensive vegetable production systems (Bai et al., 2020). The soil pH is predicted to decline further if the N fertilization and agricultural intensification continued to increase at the same rate (Zeng et al., 2017). Regarding climatic regions, the soil pH decreased mainly in humid regions, and the pH changes were not significant in other regions (Fig. 4a) mainly because of the high carbonate contents and strong buffering capacity.

The SICD have decreased by 38% and 27% at depths of 0–20 cm and 20–40 cm, respectively during the past 30 years (Fig. 2a, b). This study confirmed that soil acidification induced by N fertilization and deposition decreases SIC stocks regionally (Raza et al., 2020) and globally (Zamanian et al., 2018; Raza et al., 2021b). Globally, calcareous soils are estimated to release 7.48 Tg C as CO_2 annually from SIC due to acidification induced by N fertilizers (Zamanian et al., 2018; Zamanian and Kuzyakov, 2019). The long-term classical experiment at Rothamsted station reported that 100 years of continuous N fertilization completely removed $CaCO_3$ and that the soil became very acidic (Poulton, 1996). A 75-year field experiment in California showed that the SIC stocks in the 2 m soil profile in irrigated cropland were lower than those in non-irrigated fallow land (Eshel et al., 2007). Approximately 51% of cultivated soils in China are currently losing SIC, mainly those in the northeast region (Wu et al., 2009). The SIC contents at 0–60 cm depth were reduced after 15 years of N application on the North China Plain, and the $HCO_3^-/(Ca^{2+}+Mg^{2+})$ ratio in the leachate was higher in N-fertilized plots than in plots without N, indicating accelerated carbonate dissolution under fertilizer-induced soil acidification (Dong et al., 2016). N fertilization for 22 years reduced the SIC contents in the 1 m profile under maize compared with that under fallow land (Qiu et al., 2016). Compared with that in naturally vegetated areas, SIC storage in the 7.3 m profile in rain-fed and artificially irrigated cropland decreased over 30–100 years due to SIC dissolution and leaching (Kim et al., 2020). The SIC content in the topsoil (0–40 cm) decreased with increasing cultivation time, and SIC accumulated at depths of 120–200 cm (Wang et al., 2019). The SIC stocks in the 0–30 cm and 30–100 cm layers in a cropland were lower than those in a meadow soil (Wang et al., 2013). Nitrogen fertilization increases SOC input, which accelerates microbial activity and CO_2 emissions, which after reaction with water forms carbonic acidic and cause SIC losses (Cardinael et al., 2020). Therefore, it is clear that SIC losses are happening worldwide and in almost all land use systems.

The SICD of croplands (0–20 cm) is influenced by the water balance (P/PET). The SICD contents decreased in all areas except in arid climate areas (Fig. 4). The increase in SICD in the arid regions of Xinjiang, Gansu, and Ningxia (Fig. 6a) may have been due to: i) irrigation with brackish water containing Ca^{2+}, Mg^{2+} and HCO_3^- facilitating carbonate formation (de Soto et al., 2017; Xiao et al., 2014; Bughio et al., 2016), ii) widespread saline soils containing base cations (Ca^{2+} and Mg^{2+}) causing carbonate formation (Li et al., 2020), and (iii) lower P/PET. Above phenomena could partly explain the contrary results obtained in some studies showing SIC increase under agricultural activities and fertilization than those in soils under natural vegetation (Li et al., 2016; Mikhailova and Post, 2006; Pal et al., 2000; Wang et al., 2014; J.P. Wang et al., 2015; X. Wang et al., 2015).

Although the SICD and average pH value of Chinese cropland soils have generally decreased during the past 30 years (Figs. 6a and 4a), the changes in SICD were not always consistent with those in pH (Fig. S2b). Although SIC was greatly decreased in some areas, the pH remained stable. This is because soils with high SICD have high buffering capacity, and H^+ production in such soils is continuously buffered through SIC dissolution, and the pH value remains stable, and could partly explain the reason behind the dispersion in the data points (Fig. 3, Fig. 5). The soil pH starts decreasing significantly only when the SIC stocks are completely exhausted, at pH < 6.5 (Raza et al., 2020). Therefore, regular monitoring of the SIC content in intensive agricultural systems is recommended, especially in humid regions with high N fertilization rates.

4.2. Driving factors controlling changes in SICD

Acidification is a major driver of SICD decrease mainly through carbonate dissolution (Figs. S2a, 7f, S5). A decrease in pH can be driven by many processes, most notably by N fertilization (Raza et al., 2020). A high N input rate (560 kg N ha^{-1} yr^{-1}) for two years in a wheat-maize rotation added 13 keq of H^+ ions per ha as a result of nitrification, root nutrient uptake, and HCO_3^- leaching (Hao et al., 2019). N application for 22 years in a wheat-maize rotation reduced the pH and $CaCO_3$ contents in a calcareous soil (Zhang et al., 2016). Conservation tillage with residue application for six years in rice-wheat rotation decreased SIC stocks by 2.3 Mg ha^{-1}, which was attributed to the acidification caused by H_2CO_3, and the release of acidic metabolites during the decomposition of plant residues (Dey et al., 2020). Nitrogen-induced acidification also accelerates silicate weathering (e.g., wollastonite, $CaSiO_3$), releasing Ca^{2+} and/or Mg^{2+} (Monger et al., 2015; Koester et al., 2021), an additional Ca^{2+} can also add from irrigation water, runoff water, and dust; these cations can then react with CO_2 generated by root and microbial respiration and the decomposition of organic matter. These processes may then lead to the formation of pedogenic carbonates through the reaction of CO_2 in soil solution with Ca^{2+} and Mg^{2+} (Zamanian et al., 2016a; Landi et al., 2003; Beerling et al., 2020); consequently, the SIC contents may even increase under N fertilization in the absence of leaching and could be reason behind the dispersion of the data points (Fig. 3, Fig. 4; Beaulieu et al., 2011). This is why the soil pH remained stable in areas with low rainfall (and thus no leaching) and low N fertilizer application (Figs. 4a, 7f).

The soil water balance (P/PET) is an effective indicator for evaluating leaching (UNESCO, 1979; Yang et al., 2005). The soil pH decreased in areas with a positive water balance (Fig. 4b). In regions with P/PET >1.1, pH decreased by 0.91 units (Fig. 4a), and this decrease occurred even more rapidly with an increase in the cumulative N input (Fig. S6). In areas with high rainfall, the risk of NO_3^- leaching was significantly high. During NO_3^- leaching, Ca^{2+}, Mg^{2+} and other associated base cations are lost in order to maintain the charge balance in the soil; this process induces acidification and reduces the SIC content and buffering capacity in the topsoil (Guo et al., 2010; Gilliam et al., 2020; Aquilina et al., 2012). The intensity of rainfall events can also strongly increase SIC losses, as higher precipitation can exacerbate acidification by accelerating base cations leaching (Rengel, 2011). The soil pH had a negative correlation with P/PET in 31 soil types (Fig. S3). SICD losses occur the most rapidly in humid regions (Fig. 5, Fig. 6b, S8, S9). Although N fertilizer inputs are low in the monocropping systems in Heilongjiang and Jilin provinces, the relatively high P/PET in these areas still indicates the risk of SIC dissolution and leaching (You et al., 2020). Leptic Cambisols are the dominant soil type in Sichuan; these soils develop from the weathering of purple mudstone of the Triassic-Cretaceous system and contain carbonates (Zhang et al., 2017). The increase in carbonate contents in these soils over time could be due to the exposure of underlying deeper horizons through strong erosion (Fig. 7a, b; Quijano et al., 2020). The ΔSICD in the various soil types decreased with increasing P/PET. The SICD increase at 20–40 cm in Calcic Solonchaks may have occurred because these soils originally had large amounts of SIC, which moved downward following the implementation of agricultural practices and were redeposited at 20–40 cm.

Based on the identified driving factors, this study proposes the following trends in SICD: (1) In humid areas, soil acidification dissolves $CaCO_3$, and base cations such as Ca^{2+} are leached to below 40 cm; (2) in soils where the water input is approximately equal to or higher than the potential evapotranspiration (0.65 > P/PET > 2.0), H^+ is generated, which accelerates $CaCO_3$ dissolution, but Ca^{2+} losses through leaching are low; therefore, the SICD remains relatively stable; and (3) in arid regions, the high transpiration rates cause water to be lost from the soil, resulting in the conversion of Ca^{2+} and Mg^{2+} which come from the weathering of $CaSiO_3$ and irrigation into pedogenic carbonates; therefore, the SICD increases (Fig. 8).

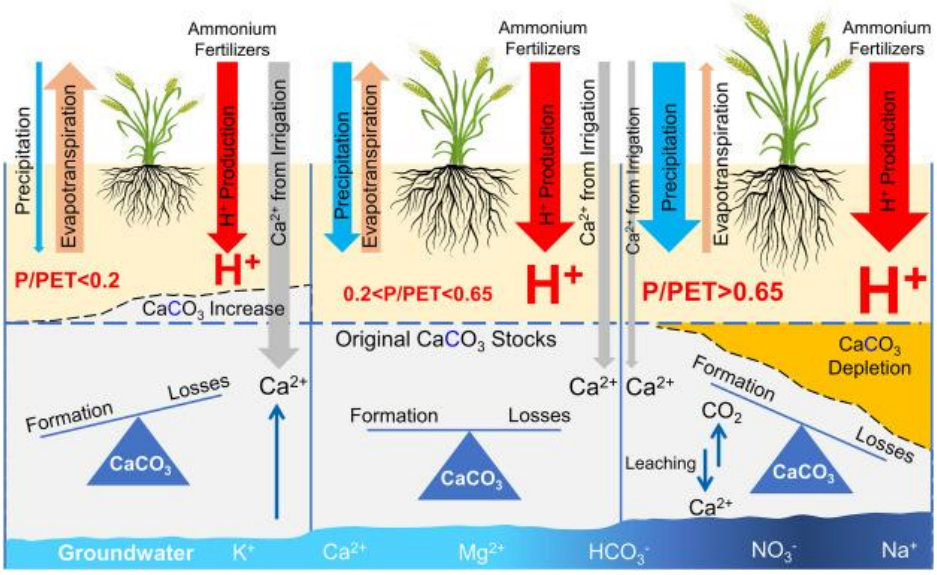

Download : Download high-res image (893KB)

Download : Download full-size image

Fig. 8. Carbonate budget (dissolution and precipitation) in agricultural soils driven by the water balance (precipitation-to-potential evapotranspiration ratio, P/PET) and acidification (H^+). The blue dashed line in the middle of the figure shows the initial $CaCO_3$ content in soils (not proportional to the climatic conditions). Nitrogen inputs, mainly from fertilization, and the subsequent H^+ production increase from arid to humid regions (minimum values in arid regions and maximum values in humid regions). The precipitation and groundwater level increase from left to right. The box on the left shows the increases in $CaCO_3$ with time because of the formation of pedogenic carbonates facilitated by Ca^{2+} input and drought. Ca^{2+} addition in arid soils comes mainly from irrigation and the upward movement of groundwater. A small fraction of the Ca^{2+} also comes from fertilizer; this fraction was considered equal in all regions. The orange area on the right represents the loss of $CaCO_3$ over time because of water input and acidification. The width of the arrows is roughly proportional to the relative value of each parameter.

4.3. Uncertainty analysis

This study was based on two types of data collection: (i) soil sampling and analysis, (ii) data collection from the literature. Paired data points were established from similar locations sampled during the 1980s and 2010s. The sample sites were described through their geographic locations because GPS was not available in the 1980s. This may have resulted in slightly different sampling locations being compared between the two time periods. This problem was addressed by comparing the parent material, soil type, and soil texture to minimize these errors, as well as by considering a large number of samples. However, there may still have been some differences between locations.

Additionally, soil erosion over 30 years may have exposed underlying soils with high carbonate content (Tong et al., 2020; Zhong et al., 2019). Therefore, erosion may increase the SIC content in the surface soil and mask the effects of N fertilizer and water inputs. This study estimated SICD only at 0–40 cm depth and did not consider SIC leaching into deeper soils. Soil acidification causes carbonate dissolution, and irrigation leads to the leaching of Ca^{2+}, which may reprecipitate in the deep layers (2–3 m) and form pedogenic carbonates (Filippi et al., 2020; Zamanian et al., 2016a, Zamanian et al., 2016b; Bughio et al., 2016). Ca^{2+} uptake by crops and Ca^{2+} inputs from fertilizers also affect the soil Ca^{2+} balance, which in turn affects the formation of pedogenic carbonates (Raza et al., 2021a).

5. Conclusions

Meeting environment sustainability goals demand increasing C sequestration and minimizing its losses to the environment. Irrigation and N fertilization have increased crops yield and SOC input to soils, but have accelerated acidification-induced SIC losses, and thus reducing the net benefits for environment. The SICD in Chinese croplands has decreased by 27–38% in the 0–40 cm soil layer, and the pH has decreased by 0.53 units over the past 30 years. The decreases in pH (0.72–0.91 units) and SICD (0.19–0.93 kg C m^{-2}) noted in this study were more pronounced in humid

and subhumid regions. The combination of N fertilization and leaching exacerbated losses of SICD and dissolved Ca^{2+}. SIC losses can deteriorate long-term soil health, crops productivity, and ecological services. Therefore, the balanced use of inputs such as N fertilization and irrigation should be performed strictly according to the requirements of crops and the soil nutrient status. Government authorities and the scientific community should increase their focus on SIC stocks, and their regular monitoring is necessary in areas with high N fertilization and precipitation.

CRediT authorship contribution statement

J.Z. conceived and designed the study with inputs from J.T. S.R., and Z.C. J.T., M.Z., J.C., P.W., and Z.C. conducted the study. S.R., J.T., J.Z., and Y.K. wrote the paper, and Y.S., K.Z., and M.X. contributed to the discussion, interpretation of results, and paper writing.

Declaration of competing interest

The authors declare that they have no known competing financial interests or personal relationships that could have appeared to influence the work reported in this paper.

Acknowledgments

We thank the National Natural Science Foundation of China (41671295), the National Key Research and Development Program of China (No. 2017YFD0200106), the 111 Project (No. B12007), the International Young Scientists Program of the National Natural Science Foundation of China (42050410320), the German Research Foundation (ZA 1068/4-1), and "RUDN University program 5-100" for their support. We greatly acknowledge the support from Prof. Yanbing Qi from Northwest A&F University, Prof. Hongjian Gao from Anhui Agricultural University, and Prof. Junfeng Ji from Nanjing University during data collection and soil sampling.

Appendix A. Supplementary data

Download : Download Word document (2MB)

Supplementary figures

Recommended articles

References

An et al., 2019 H. An, X. Wu, Y. Zhang, Z. Tang

Effects of land-use change on soil inorganic carbon: a meta-analysis

Geoderma, 353 (2019), pp. 273-282, 10.1016/j.geoderma.2019.07.008

View PDF View article View in Scopus Google Scholar

Aquilina et al., 2012 L. Aquilina, A. Poszwa, C. Walter, V. Vergnaud, A.C. Pierson-Wickmann, L. Ruiz

Long-term effects of high nitrogen loads on cation and carbon riverine export in agricultural catchments

Environ. Sci. Technol., 46 (17) (2012), pp. 9447-9455, 10.1021/es301715t

View in Scopus Google Scholar

Bai et al., 2020 X.L. Bai, J.J. Gao, S.C. Wang, H.M. Cai, Z.J. Chen, J.B. Zhou

Excessive nutrient balance surpluses in newly built solar greenhouses over five years leads to high nutrient accumulations in soil

Agric. Ecosyst. Environ., 288 (2020), Article 106717, 10.1016/j.agee.2019.106717

View PDF View article View in Scopus Google Scholar

Batjes, 1996 N.H. Batjes

Total carbon and nitrogen in the soils of the world
Eur. J. Soil Sci., 47 (2) (1996), pp. 151-163
CrossRef ↗ View in Scopus ↗ Google Scholar ↗

Beaulieu et al., 2011 E. Beaulieu, Y. Goddéris, D. Labat, C. Roelandt, D. Calmels, J. Gaillardet
Modeling of water-rock interaction in the Mackenzie basin: competition between sulfuric and carbonic acids
Chem. Geol., 289 (1) (2011), pp. 114-123, 10.1016/j.chemgeo.2011.07.020 ↗
View PDF View article View in Scopus ↗ Google Scholar ↗

Beerling et al., 2020 D.J. Beerling, E.P. Kantzas, M.R. Lomas, P. Wade, R.M. Eufrasio, P. Renforth, S.A. Banwart
Potential for large-scale CO2 removal via enhanced rock weathering with croplands
Nature, 583 (7815) (2020), pp. 242-248, 10.1038/s41586-020-2448-9 ↗
View in Scopus ↗ Google Scholar ↗

Bramble et al., 2020 D.S.E. Bramble, G.A. Gouveia, R. Ramnarine, R.E. Farrell
Short-term effects of aglime on inorganic- and organic-derived CO2 emissions from two acid soils amended with an ammonium-based fertiliser
J. Soils Sediments, 20 (1) (2020), pp. 52-65, 10.1007/s11368-019-02407-2 ↗
View in Scopus ↗ Google Scholar ↗

Bughio et al., 2016 M.A. Bughio, P. Wang, F. Meng, C. Qing, Y. Kuzyakov, X. Wang, S.A. Junejo
Neoformation of pedogenic carbonates by irrigation and fertilization and their contribution to carbon sequestration in soil
Geoderma, 262 (2016), pp. 12-19, 10.1016/j.geoderma.2015.08.003 ↗
View PDF View article View in Scopus ↗ Google Scholar ↗

Cardinael et al., 2020 R. Cardinael, T. Chevallier, B. Guenet, C. Girardin, T. Cozzi, V. Pouteau, C. Chenu
Organic carbon decomposition rates with depth and contribution of inorganic carbon to CO2 emissions under a Mediterranean agroforestry system
Eur. J. Soil Sci., 71 (5) (2020), pp. 909-923, 10.1111/ejss.12908 ↗
View in Scopus ↗ Google Scholar ↗

de Soto et al., 2017 I.S. de Soto, I. Virto, P. Barré, O. Fernández-Ugalde, R. Antón, I. Martínez, P. Bescansa
A model for field-based evidences of the impact of irrigation on carbonates in the tilled layer of semi-arid Mediterranean soils
Geoderma, 297 (2017), pp. 48-60, 10.1016/j.geoderma.2017.03.005 ↗
View PDF View article View in Scopus ↗ Google Scholar ↗

Dey et al., 2020 A. Dey, B.S. Dwivedi, R. Bhattacharyya, S.P. Datta, M.C. Meena, R.K. Jat, R.G. Singh, ...
Effect of conservation agriculture on soil organic and inorganic carbon sequestration and lability: a study from a rice–wheat cropping system on a calcareous soil of the eastern indo-Gangetic Plains
Soil Use Manag., 36 (3) (2020), pp. 429-438, 10.1111/sum.12577 ↗
View in Scopus ↗ Google Scholar ↗

Dong et al., 2016 W. Dong, Y. Duan, Y. Wang, C. Hu
Reassessing carbon sequestration in the North China plain via addition of nitrogen
Sci. Total Environ., 563–564 (2016), pp. 138-144, 10.1016/j.scitotenv.2016.04.115 ↗
View PDF View article View in Scopus ↗ Google Scholar ↗

Eshel et al., 2007 G. Eshel, P. Fine, M.J. Singer
Total soil carbon and water quality: an implication for carbon sequestration
Soil Sci. Soc. Am. J., 71 (2) (2007), pp. 397-405, 10.2136/sssaj2006.0061 ↗

View in Scopus ↗ Google Scholar ↗

Filippi et al., 2020 P. Filippi, S.R. Cattle, M.J. Pringle, T.F.A. Bishop

A two-step modelling approach to map the occurrence and quantity of soil inorganic carbon

Geoderma, 371 (2020), Article 114382, 10.1016/j.geoderma.2020.114382 ↗

View PDF View article View in Scopus ↗ Google Scholar ↗

Fowler et al., 2013 D. Fowler, M. Coyle, U. Skiba, M.A. Sutton, J.N. Cape, S. Reis, J.N. Galloway

The global nitrogen cycle in the twenty-first century

Philos. Trans. R. Soc., B, 368 (1621) (2013), Article 20130164

CrossRef ↗ View in Scopus ↗ Google Scholar ↗

Gai et al., 2018 X. Gai, H. Liu, J. Liu, L. Zhai, B. Yang, S. Wu, H. Wang, ...

Long-term benefits of combining chemical fertilizer and manure applications on crop yields and soil carbon and nitrogen stocks in North China Plain

Agric. Water Manag., 208 (2018), pp. 384-392, 10.1016/j.agwat.2018.07.002 ↗

View PDF View article View in Scopus ↗ Google Scholar ↗

Gile et al., 1966 L.H. Gile, F.F. Peterson, R.B. Grossman

Morphological and genetic sequences of carbonate accumulation in desert soils

Soil Sci., 101 (5) (1966), pp. 347-360, 10.1097/00010694-196605000-00001 ↗

View in Scopus ↗ Google Scholar ↗

Gilliam et al., 2020 F.S. Gilliam, M.B. Adams, W.T. Peterjohn

Response of soil fertility to 25 years of experimental acidification in a temperate hardwood forest

J. Environ. Qual., 49 (4) (2020), pp. 961-972, 10.1002/jeq2.20113 ↗

View in Scopus ↗ Google Scholar ↗

Gocke & Kuzyakov, 2011 M. Gocke, Y. Kuzyakov

Effect of temperature and rhizosphere processes on pedogenic carbonate recrystallization: relevance for paleoenvironmental applications

Geoderma, 166 (1) (2011), pp. 57-65, 10.1016/j.geoderma.2011.07.011 ↗

View PDF View article View in Scopus ↗ Google Scholar ↗

Guo et al., 2010 J.H. Guo, X.J. Liu, Y. Zhang, J.L. Shen, W.X. Han, W.F. Zhang, F.S. Zhang

Significant acidification in major Chinese Croplands

Science, 327 (5968) (2010)

doi:1008-1010.10.1126/science.1182570

Google Scholar ↗

Han et al., 2018 X. Han, G. Gao, R. Chang, Z. Li, Y. Ma, S. Wang, B. Fu, ...

Changes in soil organic and inorganic carbon stocks in deep profiles following cropland abandonment along a precipitation gradient across the Loess Plateau of China

Agric. Ecosyst. Environ., 258 (2018), pp. 1-13, 10.1016/j.agee.2018.02.006 ↗

View PDF View article Google Scholar ↗

Hao et al., 2019 T. Hao, Q. Zhu, M. Zeng, J. Shen, X. Shi, X. Liu, W. de Vries, ...

Quantification of the contribution of nitrogen fertilization and crop harvesting to soil acidification in a wheat-maize double cropping system

Plant Soil, 434 (1) (2019), pp. 167-184

CrossRef ↗ View in Scopus ↗ Google Scholar ↗

Hein et al., 2020 C.J. Hein, M. Usman, T.I. Eglinton, N. Haghipour, V.V. Galy

Millennial-scale hydroclimate control of tropical soil carbon storage

Nature, 581 (7806) (2020), pp. 63-66, 10.1038/s41586-020-2233-9 ↗

View in Scopus ↗ Google Scholar ↗

Jones & Reid, 2001 P.D. Jones, P.A. Reid

Temperature trends in regions affected by increasing aridity/humidity

Geophys. Res. Lett., 28 (20) (2001), pp. 3919-3922, 10.1029/2001GL013840 ↗

View in Scopus ↗ Google Scholar ↗

Kim et al., 2020 J.H. Kim, E.G. Jobbagy, D.D. Richter, S.E. Trumbore, R.B. Jackson

Agricultural acceleration of soil carbonate weathering

Glob. Chang. Biol., 26 (10) (2020), pp. 5988-6002, 10.1111/gcb.15207 ↗

View in Scopus ↗ Google Scholar ↗

Koester et al., 2021 M. Koester, S.C. Stock, F. Nájera, K. Abdallah, A. Gorbushina, J. Prietzel, S. Spielvogel, ...

From rock eating to vegetarian ecosystems — disentangling processes of phosphorus acquisition across biomes

Geoderma, 388 (2021), Article 114827, 10.1016/j.geoderma.2020.114827 ↗

View PDF View article View in Scopus ↗ Google Scholar ↗

Kuzyakov et al., 2021 Y. Kuzyakov, I. Kuzyakova, S. Raza, J. Zhou, K. Zamanian

Letter-to-the-editor: does acidification really increase soil carbon in croplands? How statistical analyses of large datasets might mislead the conclusions

Geoderma, 384 (2021), Article 114806, 10.1016/j.geoderma.2020.114806 ↗

View PDF View article View in Scopus ↗ Google Scholar ↗

Landi et al., 2003 A. Landi, A.R. Mermut, D.W. Anderson

Origin and rate of pedogenic carbonate accumulation in Saskatchewan soils, Canada

Geoderma, 117 (1) (2003), pp. 143-156, 10.1016/S0016-7061(03)00161-7 ↗

View PDF View article View in Scopus ↗ Google Scholar ↗

Li et al., 2007 Z.P. Li, F.X. Han, Y. Su, T.L. Zhang, B. Sun, D.L. Monts, M.J. Plodinec

Assessment of soil organic and carbonate carbon storage in China

Geoderma, 138 (1) (2007), pp. 119-126, 10.1016/j.geoderma.2006.11.007 ↗

View PDF View article Google Scholar ↗

Li et al., 2016 C. Li, Q. Li, L. Zhao, S. Ge, D. Chen, Q. Dong, X. Zhao

Land-use effects on organic and inorganic carbon patterns in the topsoil around Qinghai Lake basin, Qinghai-tibetan plateau

Catena, 147 (2016), pp. 345-355, 10.1016/j.catena.2016.07.040 ↗

View PDF View article View in Scopus ↗ Google Scholar ↗

Li et al., 2017 Y. Li, C. Zhang, N. Wang, Q. Han, X. Zhang, Y. Liu, W. Ye, ...

Substantial inorganic carbon sink in closed drainage basins globally

Nat. Geosci., 10 (7) (2017), pp. 501-506, 10.1038/ngeo2972 ↗

View PDF View article Google Scholar ↗

Li et al., 2020 L. Li, H. Liu, X. He, E. Lin, G. Yang

Winter irrigation effects on soil moisture, temperature and salinity, and on cotton growth in salinized fields in northern Xinjiang, China

Sustainability (Basel, Switzerland), 12 (18) (2020), p. 7573, 10.3390/su12187573 ↗

View in Scopus ↗ Google Scholar ↗

Liu et al., 2020 S. Liu, L. Zhou, H. Li, X. Zhao, Y. Yang, Y. Zhu, P. Kardol, ...

Shrub encroachment decreases soil inorganic carbon stocks in Mongolian grasslands

J. Ecol., 108 (2) (2020), pp. 678-686, 10.1111/1365-2745.13298

View in Scopus Google Scholar

Loisel et al., 2019 J. Loisel, C.J. Casellas, G. Hugelius, J.W. Harden, C.L. Morgan

Soils can help mitigate CO2 emissions, despite the challenges

Proc. Natl Acad. Sci. USA, 116 (21) (2019), pp. 10211-10212

https://doi.org/10.1073/pnas.1900444116

CrossRef View in Scopus Google Scholar

Lu et al., 2020 T. Lu, X. Wang, M. Xu, Z. Yu, Y. Luo, P. Smith

Dynamics of pedogenic carbonate in the cropland of the North China plain: influences of intensive cropping and salinization

Agric. Ecosyst. Environ., 292 (2020), Article 106820, 10.1016/j.agee.2020.106820

View PDF View article View in Scopus Google Scholar

Mikhailova & Post, 2006 E.A. Mikhailova, C.J. Post

Effects of land use on soil inorganic carbon stocks in the russian chernozem

J. Environ. Qual., 35 (4) (2006), pp. 1384-1388, 10.2134/jeq2005.0151

View in Scopus Google Scholar

Monger et al., 2015 H.C. Monger, R.A. Kraimer, S.E. Khresat, D.R. Cole, X. Wang, J. Wang

Sequestration of inorganic carbon in soil and groundwater

Geology, 43 (5) (2015), pp. 375-378, 10.1130/G36449.1

Google Scholar

National Bureau of Statistics of China (NBSC), 2016 National Bureau of Statistics of China (NBSC)

China agriculture yearbook

Retrieved from

China Agriculture Press, Beijing (2016)

http://www.stats.gov.cn/english/

Google Scholar

National Soil Survey Office of China, 1994 National Soil Survey Office of China

China Soil Species

Vols. 1–6, China Agriculture Press, Beijing, China (1994)

Google Scholar

NMDC (National Meteorological Data Center, 2019 NMDC (National Meteorological Data Center

Beijing, China

Accessible at

http://data.cma.cn/ (2019)

Google Scholar

Pal et al., 2000 D.K. Pal, G.S. Dasog, S. Vadivelu, R.L. Ahuja, T. Bhattacharyya

Secondary calcium carbonate in soils of arid and semi-arid regions of India

Global Climate Change and Pedogenic Carbonates (2000), pp. 149-185

View in Scopus Google Scholar

Post & Kwon, 2000 W.M. Post, K.C. Kwon

Soil carbon sequestration and land-use change: processes and potential

Glob. Chang. Biol., 6 (3) (2000), pp. 317-327

View in Scopus Google Scholar

Poulton, 1996 P.R. Poulton

Management and modification procedures for long-term field experiments
Can. J. Plant Sci., 76 (4) (1996), pp. 587-594
CrossRef ↗ View in Scopus ↗ Google Scholar ↗

Qiu et al., 2016 S. Qiu, H. Gao, P. Zhu, Y. Hou, S. Zhao, X. Rong, W. Zhou, ...
Changes in soil carbon and nitrogen pools in a Mollisol after long-term fallow or application of chemical fertilizers, straw or manures
Soil Tillage Res., 163 (2016), pp. 255-265, 10.1016/j.still.2016.07.002 ↗
View PDF View article View in Scopus ↗ Google Scholar ↗

Quade & Cerling, 1990 J. Quade, T.E. Cerling
Stable isotopic evidence for a pedogenic origin of carbonates in trench 14 near Yucca Mountain, Nevada
Science, 250 (4987) (1990), pp. 1549-1552, 10.1126/science.250.4987.1549 ↗
View in Scopus ↗ Google Scholar ↗

Quijano et al., 2020 L. Quijano, N.J. Kuhn, A. Navas
Effects of interrill erosion on the distribution of soil organic and inorganic carbon in different sized particles of Mediterranean calcisols
Soil Tillage Res., 196 (2020), Article 104461, 10.1016/j.still.2019.104461 ↗
View PDF View article View in Scopus ↗ Google Scholar ↗

Raheb et al., 2017 A. Raheb, A. Heidari, S. Mahmoodi
Organic and inorganic carbon storage in soils along an arid to dry sub-humid climosequence in northwest of Iran
Catena (Giessen), 153 (2017), pp. 66-74, 10.1016/j.catena.2017.01.035 ↗
View PDF View article View in Scopus ↗ Google Scholar ↗

Raza et al., 2020 S. Raza, N. Miao, P.Z. Wang, X.T. Ju, Z.J. Chen, J.B. Zhou, Y. Kuzyakov
Dramatic loss of inorganic carbon by nitrogen-induced soil acidification in Chinese croplands
Glob. Chang. Biol., 26 (6) (2020), pp. 3738-3751, 10.1111/gcb.15101 ↗
View in Scopus ↗ Google Scholar ↗

Raza et al., 2021a S. Raza, Y. Kuzyakov, J.B. Zhou
Facts to acidification-induced carbonate losses from chinese croplands
Glob. Chang. Biol., 27 (5) (2021), 10.1111/gcb.15478 ↗
Google Scholar ↗

Raza et al., 2021b S. Raza, K. Zamanian, S. Ullah, Y. Kuzyakov, I. Virto, J. Zhou
Inorganic carbon losses by soil acidification jeopardize global efforts on carbon sequestration and climate change mitigation
J. Clean. Prod. (2021), Article 128036, 10.1016/j.jclepro.2021.128036 ↗
View PDF View article View in Scopus ↗ Google Scholar ↗

Rengel, 2011 Z. Rengel
Soil pH, soil health and climate change
Soil Health and Climate Change, Springer, Berlin, Heidelberg (2011), pp. 69-85, 10.1007/978-3-642-20256-8_4 ↗
View in Scopus ↗ Google Scholar ↗

Rowley et al., 2020 M.C. Rowley, S. Grand, T. Adatte, E.P. Verrecchia
A cascading influence of calcium carbonate on the biogeochemistry and pedogenic trajectories of subalpine soils, Switzerland
Geoderma, 361 (2020), Article 114065, 10.1016/j.geoderma.2019.114065 ↗

View PDF View article View in Scopus ↗ Google Scholar ↗

Schlesinger, 1982 W.H. Schlesinger

Carbon storage in the caliche of arid soils: a case study from Arizona

Soil Sci., 133 (4) (1982), pp. 247-255, 10.1097/00010694-198204000-00008 ↗

View in Scopus ↗ Google Scholar ↗

Schlesinger, 1985 W.H. Schlesinger

The formation of caliche in soils of the Mojave Desert, California

Geochim. Cosmochim. Acta, 49 (1) (1985), pp. 57-66, 10.1016/0016-7037(85)90191-7 ↗

View PDF View article View in Scopus ↗ Google Scholar ↗

Shi et al., 2012 Y. Shi, F. Baumann, Y. Ma, C. Song, P. Kühn, T. Scholten, J. He

Organic and inorganic carbon in the topsoil of the Mongolian and Tibetan grasslands: pattern, control and implications

Biogeosciences, 9 (6) (2012), pp. 2287-2299

CrossRef ↗ View in Scopus ↗ Google Scholar ↗

Sinha et al., 2017 E. Sinha, A.M. Michalak, V. Balaji

Eutrophication will increase during the 21st century as a result of precipitation changes

Science, 357 (6349) (2017), pp. 405-408, 10.1126/science.aan2409 ↗

Google Scholar ↗

Slessarev et al., 2016 E.W. Slessarev, Y. Lin, N.L. Bingham, J.E. Johnson, Y. Dai, J.P. Schimel, O.A. Chadwick

Water balance creates a threshold in soil pH at the global scale

Nature, 540 (7634) (2016), pp. 567-569, 10.1038/nature20139 ↗

View in Scopus ↗ Google Scholar ↗

Steffen et al., 2015 W. Steffen, K. Richardson, J. Rockström, S.E. Cornell, I. Fetzer, E.M. Bennett, C.A. De Wit, ...

Planetary boundaries: guiding human development on a changing planet

Science, 347 (6223) (2015)

Google Scholar ↗

Tan et al., 2014 W. Tan, R. Zhang, H. Cao, C. Huang, Q. Yang, M. Wang, L.K. Koopal

Soil inorganic carbon stock under different soil types and land uses on the loess plateau region of China

Catena (Giessen), 121 (2014), pp. 22-30, 10.1016/j.catena.2014.04.014 ↗

View PDF View article View in Scopus ↗ Google Scholar ↗

Tian & Niu, 2015 D. Tian, S. Niu

A global analysis of soil acidification caused by nitrogen addition

Environ. Res. Lett., 10 (2) (2015), p. 24019, 10.1088/1748-9326/10/2/024019 ↗

Google Scholar ↗

Tong et al., 2020 L.S. Tong, N.F. Fang, H.B. Xiao, Z.H. Shi

Sediment deposition changes the relationship between soil organic and inorganic carbon: evidence from the Chinese loess plateau

Agric. Ecosyst. Environ., 302 (2020), Article 107076, 10.1016/j.agee.2020.107076 ↗

View PDF View article View in Scopus ↗ Google Scholar ↗

UNESCO, 1979 UNESCO

Map of the world distribution of arid regions

Man and Biosphere Tech Notes, No. 7, UNESCO, Paris (1979), p. 54

View in Scopus ↗ Google Scholar ↗

Wang et al., 2013 Z. Wang, X. Han, S.X. Chang, B. Wang, Q. Yu, L. Hou, L. Li
Soil organic and inorganic carbon contents under various land uses across a transect of continental steppes in Inner Mongolia
Catena (Giessen), 109 (2013), pp. 110-117, 10.1016/j.catena.2013.04.008
View PDF View article Google Scholar

Wang et al., 2014 X.J. Wang, M.G. Xu, J.P. Wang, W.J. Zhang, X.Y. Yang, S.M. Huang, H. Liu
Fertilization enhancing carbon sequestration as carbonate in arid cropland: assessments of long-term experiments in northern China
Plant Soil, 380 (1/2) (2014), pp. 89-100, 10.1007/s11104-014-2077-x
Google Scholar

Wang et al., 2015 C. Wang, W. Li, Z. Yang, Y. Chen, W. Shao, J. Ji
An invisible soil acidification: critical role of soil carbonate and its impact on heavy metal bioavailability
Sci. Rep., 5 (2015), p. 12735, 10.1038/srep12735
View in Scopus Google Scholar

Wang et al., 2015 J.P. Wang, X.J. Wang, J. Zhang, C.Y. Zhao
Soil organic and inorganic carbon and stable carbon isotopes in the Yanqi Basin of northwestern China
Eur. J. Soil Sci., 66 (1) (2015), pp. 95-103, 10.1111/ejss.12188
View PDF View article Google Scholar

Wang et al., 2015 X. Wang, J. Wang, M. Xu, W. Zhang, T. Fan, J. Zhang
Carbon accumulation in arid croplands of Northwest China: pedogenic carbonate exceeding organic carbon
Sci. Rep., 5 (2015), p. 11439, 10.1038/srep11439
View in Scopus Google Scholar

Wang et al., 2019 Y. Wang, J. Jiang, Z. Niu, Y. Li, C. Li, W. Feng
Responses of soil organic and inorganic carbon vary at different soil depths after long-term agricultural cultivation in Northwest China
Land Degrad. Dev., 30 (10) (2019), pp. 1229-1242, 10.1002/ldr.3311
View in Scopus Google Scholar

Wu et al., 2009 H. Wu, Z. Guo, Q. Gao, C. Peng
Distribution of soil inorganic carbon storage and its changes due to agricultural land use activity in China
Agric. Ecosyst. Environ., 129 (4) (2009), pp. 413-421, 10.1016/j.agee.2008.10.020
View PDF View article View in Scopus Google Scholar

Xiao et al., 2014 J. Xiao, Z. Jin, J. Wang
Assessment of the hydrogeochemistry and groundwater quality of the Tarim River Basin in an extreme arid region, NW China
Environ. Manag., 53 (1) (2014), pp. 135-146, 10.1007/s00267-013-0198-2
View in Scopus Google Scholar

Xie et al., 2019 E. Xie, Y. Zhao, H. Li, X. Shi, F. Lu, X. Zhang, Y. Peng
Spatio-temporal changes of cropland soil pH in a rapidly industrializing region in the Yangtze River Delta of China, 1980–2015
Agric. Ecosyst. Environ., 272 (2019), pp. 95-104, 10.1016/j.agee.2018.11.015
View PDF View article View in Scopus Google Scholar

Yang et al., 2005 J. Yang, Y. Ding, R. Chen, L. Liu
Fluctuations of the semi-arid zone in China, and consequences for society
Clim. Chang., 72 (1) (2005), pp. 171-188, 10.1007/s10584-005-6858-3 ↗
View in Scopus ↗ Google Scholar ↗

Yang et al., 2010 Y. Yang, J. Fang, C. Ji, W. Ma, S. Su, Z. Tang
Soil inorganic carbon stock in the Tibetan alpine grasslands
Glob. Biogeochem. Cycles, 24 (4) (2010), Article GB4022
View in Scopus ↗ Google Scholar ↗

Yang et al., 2012 Y. Yang, J. Fang, C. Ji, W. Ma, A. Mohammat, S. Wang, P. Smith, ...
Widespread decreases in topsoil inorganic carbon stocks across China's grasslands during 1980s–2000s
Glob. Chang. Biol., 18 (12) (2012), pp. 3672-3680, 10.1111/gcb.12025 ↗
View in Scopus ↗ Google Scholar ↗

You et al., 2020 M. You, X. Han, N. Hu, S. Du, T.A. Doane, L. Li
Profile storage and vertical distribution (0–150 cm) of soil inorganic carbon in croplands in Northeast China
Catena (Giessen), 185 (2020), Article 104302, 10.1016/j.catena.2019.104302 ↗
View PDF View article View in Scopus ↗ Google Scholar ↗

Zamanian & Kuzyakov, 2019 K. Zamanian, Y. Kuzyakov
Contribution of soil inorganic carbon to atmospheric CO2: more important than previously thought
Glob. Chang. Biol., 25 (1) (2019), pp. e1-e3, 10.1111/gcb.14463 ↗
View in Scopus ↗ Google Scholar ↗

Zamanian et al., 2016a K. Zamanian, K. Pustovoytov, Y. Kuzyakov
Pedogenic carbonates: forms and formation processes
Earth Sci. Rev., 157 (2016), pp. 1-17, 10.1016/j.earscirev.2016.03.003 ↗
View PDF View article View in Scopus ↗ Google Scholar ↗

Zamanian et al., 2016b K. Zamanian, K. Pustovoytov, Y. Kuzyakov
Cation exchange retards shell carbonate recrystallization: consequences for dating and paleoenvironmental reconstructions
Catena (Giessen), 142 (2016), pp. 134-138, 10.1016/j.catena.2016.03.012 ↗
View PDF View article View in Scopus ↗ Google Scholar ↗

Zamanian et al., 2018 K. Zamanian, M. Zarebanadkouki, Y. Kuzyakov
Nitrogen fertilization raises CO2 efflux from inorganic carbon: a global assessment
Glob. Chang. Biol., 24 (7) (2018), pp. 2810-2817, 10.1111/gcb.14148 ↗
View in Scopus ↗ Google Scholar ↗

Zeng et al., 2017 M. Zeng, W. de Vries, L.T. Bonten, Q. Zhu, T. Hao, X. Liu, J. Shen, ...
Model-based analysis of the long-term effects of fertilization management on cropland soil acidification
Environ. Sci. Technol., 51 (7) (2017), pp. 3843-3851, 10.1021/acs.est.6b05491 ↗
View in Scopus ↗ Google Scholar ↗

Zhang et al., 2016 Y. Zhang, S. Zhang, R. Wang, J. Cai, Y. Zhang, H. Li, Y. Jiang, ...
Impacts of fertilization practices on pH and the pH buffering capacity of calcareous soil
Soil Sci. Plant Nutr., 62 (5–6) (2016), pp. 432-439, 10.1080/00380768.2016.1226685 ↗
View in Scopus ↗ Google Scholar ↗

Zhang et al., 2017 Y. Zhang, W. de Vries, B.W. Thomas, X. Hao, X. Shi

Impacts of long-term nitrogen fertilization on acid buffering rates and mechanisms of a slightly calcareous clay soil

Geoderma, 305 (2017), pp. 92-99, 10.1016/j.geoderma.2017.05.021

View PDF View article Google Scholar

Zhao et al., 2020 Q.Y. Zhao, S.J. Xu, W.S. Zhang, Z. Zhang, Z. Yao, X.P. Chen, C.Q. Zou

Identifying key drivers for geospatial variation of grain micronutrient concentrations in major maize production regions of China

Environ. Pollut., 266 (Pt 2) (2020), Article 115114, 10.1016/j.envpol.2020.115114

View PDF View article View in Scopus Google Scholar

Zhong et al., 2019 S. Zhong, Z. Han, J. Du, E. Ci, J. Ni, D. Xie, C. Wei

Relationships between the lithology of purple rocks and the pedogenesis of purple soils in the Sichuan Basin, China

Sci. Rep., 9 (1) (2019), p. 13272, 10.1038/s41598-019-49687-9

View in Scopus Google Scholar

Cited by (3)

Improving spectral estimation of soil inorganic carbon in urban and suburban areas by coupling

and the impact of climate change

2023, Advances in Agronomy

Show abstract

Comparable Increasing Rate of Soil Inorganic Carbon with Soil Organic Carbon after Land-Use Change Across China's Drylands

2022, SSRN

1 Jingjing Tao and Sajjad Raza are equal main-authors.

View Abstract